Supporting Information

Hoshii et al. 10.1073/pnas.1320265111

SI Materials and Methods

Mice. *Raptor*^{flox} mice (1) were crossed with *Rosa26-CreER*^{T2} (obtained from Tyler Jacks, Massachusetts Institute of Technology, Cambridge, MA) (2), *LSL-Kras*^{G12D} mice (obtained from the Mouse Models of Human Cancers Consortium of NCI at Frederick) (3), *Lck-Cre* mice (4), and *Rosa26-tdRFP* mice (5). *mTOR*^{flox} mice, *Rictor*^{flox} mice (6), and *Tsc1*^{flox} mice (obtained from the Jackson Laboratory and backcrossed for at least six generations into the C57BL/6-CD45.2 genetic background) (7) were crossed with *Rosa26-CreER*^{T2} mice. Analyses following tamoxifen (TAM) injection and collection of adult hematopoietic cells were performed when the mice were 8–10 wk old. C57BL/6-CD45.1 mice (8–12 wk old; Sankyo Lab) were used as transplantation recipients in this study. To generate mTOR^{flox} mice, we constructed a targeting vector with loxP sites flanking exon 47 of the mTOR gene and FRT recombination sites flanking a neomycin selection cassette. A diphtheria toxin cassette was added downstream of the 3′ arm to reduce the frequency of random insertion. This vector was electroporated into feeder-free TT2 ES cells, and mice with a targeted *mTOR*^{flox} allele were established using the same strategy as we used for *Raptor*^{flox} mice (1). *mTOR*^{flox} mice were also backcrossed for at least six generations into the C57BL/6-CD45.2 genetic background. The primers used to identify the mTOR alleles in PCR analyses were mtor-a (5′-CTTTGATCAGTCCTCTCAGAACCC-3′), mtor-b (5′-CAGTTCCCAAGGGATCCACC-3′), and mtor-c (5′-GGAACTTCGATCCGGAACCC-3′). All animal experiments were performed in accordance with the guidelines for animal and recombinant DNA experiments of Kanazawa University, Kansai Medical University, or Kumamoto University.

Gene Expression Profiling. Total RNA was purified by using the RNeasy Mini Kit (Qiagen) with on-column DNase treatment (Qiagen) and reverse-transcribed with an Advantage RT for PCR Kit (Clontech) following the manufacturer's instructions. The quantity of cDNA fragments was evaluated with a TaqMan Gene expression assay (Applied Biosystems). Real-time PCR was performed with Mx3000P (Stratagene) or the ViiA 7 Real-time PCR system (Applied Biosystems).

In Vitro T-Cell Differentiation. Purified Lineage$^-$Sca-1$^+$c-KIT$^+$ (LSK) cells (1×10^3) from 8- to 12-wk-old mice were cultivated for 11–16 d with TSt-4/DLL1 stromal cells (8). Cells expressing the *Rosa26-CreER*^{T2} gene were used as controls to exclude the effect of Cre activation. 4-hydroxytamoxifen (4-OHT) (Sigma) was added for the first week. Suspension cells were dissociated by pipetting and analyzed with flow cytometry.

Tamoxifen and Rapamycin Treatments. TAM (Sigma) was dissolved in corn oil (Sigma) to 20 mg/mL and injected i.p. at 150 mg/kg per day for 5 consecutive days. For TAM treatment of cells in vitro, 1 μM 4-OHT was added to the culture medium. Rapamycin (Sirolimus; LC Laboratories) was dissolved in ethanol. For in vivo experiments, the rapamycin stock solution was diluted to make a final concentration of 0.4 or 0.8 mg/mL rapamycin in 5% PEG-400, 5% Tween 80, and 4% ethanol. Rapamycin (4 or 8 mg/kg) or vehicle (5% PEG-400, 5% Tween 80, and 4% ethanol) was injected i.p. every other day.

Flow Cytometry. Monoclonal antibodies (Abs) recognizing the following cell-surface markers were used for flow cytometry: Sca-1 (E13-161.7), CD4 (L3T3), CD8 (53-6.7), B220 (RA3-6B2), TER119 (Ly-76), Gr-1 (RB6-8C5), Mac-1 (M1/70), IL7Rα chain (B12-1), FcγIII/II receptor (2.4G2), CD34 (RAM34), IgM (II/41), CD45.1 (A20), CD45.2 (104), CD25 (PC61), CD44 (IM7), and c-KIT (2B8) (all from BD Biosciences or eBiosciences). Apoptosis was evaluated with Annexin V (BD Biosciences). Marker analyses were performed using a FACSCanto II (BD Biosciences) and MACSQuantII (Miltenyi Biotec), and cell sorting was performed using a FACSAria (BD Biosciences).

For analysis of intracellular proteins, cells were fixed and stained as described previously (1). Alexa488-conjugated anti–phospho-S6 (S235/236, #4803) Ab, anti–phospho-4E-BP1 (T37/46; T36/T45 for *Mus musculus*, #2846) Ab, rabbit mAb IgG isotype control (#2975, all from Cell Signaling Technology), PE-conjugated anti–K_i-67 Ab, and mouse mAb IgG isotype control (BD Biosciences) were used. Immunostained cells were washed with 5% FBS/PBS containing Hoechst33342 and analyzed with flow cytometry.

Competitive Repopulation Assay in Vivo. Tester whole bone marrow (WBM; 1×10^6, CD45.2) and competitor WT-WBM (1×10^6, CD45.1 or CD45.1/2) were transplanted into lethally irradiated (9.5 Gy) recipient mice (CD45.1). At 4 or 8 wk after transplantation, TAM was administered to the recipients as described above. Hematopoietic cells regenerated from tester cells or competitor cells were examined with flow cytometry.

Gene Transduction by Retroviral Infection. The Myc-tagged murine Notch1 intracellular domain (NICD) DNA fragment (a gift of Shigeru Chiba, Tsukuba University, Tsukuba, Japan) was cloned into the pGCDNsam-ires-*eGFP* vector (a gift of Masafumi Onodera, National Center for Child Health and Development, Tokyo). Retroviral packaging cells (Plat-E, the kind gift of Toshio Kitamura, University of Tokyo, Tokyo) were transiently transfected with the above plasmids using X-tremegene HP (Roche), and culture supernatants containing retroviruses were collected 48 h after transfection. For the T-cell acute lymphoblastic leukemia (T-ALL) model, freshly isolated bone marrow (BM) cells from mice were suspended in RPMI medium 1640 supplemented with 20 ng/mL rmSCF, 10 ng/mL rmIL3, 10 ng/mL rmIL6, and 10 ng/mL rmIL7. After 24 h of cultivation, spin infection was performed by adding retrovirus carrying NICD-ires-GFP to the suspended cells and centrifuging at $1{,}500 \times g$ for 1 h. Then 2×10^6 infected cells were cultured for an additional 2 h and transplanted into lethally irradiated (9.5 Gy) syngeneic recipient mice along with an equal number of bone marrow cells from wild-type mice.

Secondary Transplantation of Oncogenic Kras-Evoked T-ALL Cells. Thymocytes containing T-ALL cells were collected from recipient mice (CD45.1) with oncogenic Kras-expressing donor cells (Fig. S8 *A*–*C*), and the genetic mutation in the genomic DNA encoding the PEST domain of Notch1 gene was analyzed with PCR-based DNA sequencing. Thymocytes containing T-ALL cells (5×10^5, CD45.2) and competitor WT-WBM (5×10^5, CD45.1) were transplanted into lethally irradiated (9.5 Gy) recipient mice (CD45.1). Rapamycin (4 mg/kg) or vehicle was injected i.p. every other day (Fig. 4*A*).

Immunoblotting. Cells (2×10^4 to 5×10^4) of various subpopulations were purified by cell sorting and lysed in SDS sample buffer containing protease inhibitor (P8340, Sigma), phosphatase inhibitor mixture 2 (P5726, Sigma), and phosphatase inhibitor mixture 3 (P0044, Sigma). Lysis was completed via ultrasonication, and proteins were denatured by boiling. Denatured proteins were

separated on a 5–20% acrylamide gradient gel (Wako) and transferred to a PVDF membrane (GE Healthcare). Blots were incubated with Abs against Raptor (#2280), mTOR (#2983), Rictor (#2114), phospho-4E-BP1 (T37/46; T36/T45 for *M. musculus*, #2855), 4E-BP1 (#9644), phospho-S6 (S235/236, #4858), S6 (#2217), phospho-p70S6K (T389, #9234), p70S6K (#2708), phospho-AKT (S473, #4058), AKT (#4685), Mcl-1 (#5453), Bcl-xL (#2764), Bcl-2 (#2870), PARP (#9532), cleaved Caspase-9 (#9509), Cyclin D1 (#2926), Cyclin D3 (#2936), CDK1 (#9112), CDK6 (#3136), Histone H3 (#4499) (all from Cell Signaling Technology), Cyclin D2 (sc-181, Santa Cruz Biotechnology) and β-actin (A5441, Sigma). Immunocomplexes were labeled using an HRP-conjugated anti-mouse Ab (GE Healthcare) or anti-rabbit Ab (Cell Signaling Technology) and visualized using Immunostar LD (Wako) with ImageQuant LAS 4000 (GE Healthcare).

Blood Collection and Analysis. Total BM cells were obtained from femoral and tibial bones by aspiration. Thymocytes or splenocytes were isolated by pressing the tissues through a cell strainer (BD Falcon). Mononuclear cells (MNCs) were isolated by density gradient centrifugation using Lymphoprep (Axis-Shield). Peripheral blood (PB) cells were collected from the postorbital vein and suspended in diluted heparin solution. Blood counts were performed using CellTac (Nihon Kohden). MNCs in PB were isolated by dextran sedimentation and ammonium chloride lysis of erythrocytes using standard procedures.

PCR Analysis of T-Cell Receptor β Gene Rearrangements. The analysis of T-cell receptor β (TCRβ) gene rearrangements was performed as described previously (9, 10). Genomic DNA samples were prepared from thymic double-negative (DN) and BM Mac-1$^+$ cells by alkaline lysis with NaOH. The PCR reactions were performed with Ex Taq (TaKaRa), and amplified DNA products were separated in a 1.2% agarose gel containing ethidium bromide.

Protein Synthesis Assay. Sorted Lineage-Sca-1-c-KIT+ cells (3×10^4) were cultured with methionine-free RPMI medium 1640 containing 50 μM homopropargylglycine (HPG) for 1 h. Incorporated HPG was evaluated with a Click-iT HPG Alexa Fluor 488 Protein Synthesis Kit (Life Technologies) in accordance with the manufacturer's instructions. Fluorescence was detected by MACSQuantII (Miltenyi Biotec), and median fluorescence intensity was analyzed with FlowJo (Tree Star, Inc.).

Histochemical and Immunohistochemical Staining. For May-Grünwald-Giemsa staining, PB samples or cells purified by cell sorting were attached to glass slides and stained with May-Grünwald solution (MUTO Pure Chemicals) for 3 min. Subsequently, the slides were washed with distilled water for 3 min and stained with Giemsa solution (MUTO Pure Chemicals) for 10 min. For hematoxylin–eosin staining, rehydrated paraffin-embedded tissue sections were stained with Mayer's hematoxylin solution (Wako) for 5 min and washed with water for 5 min. The slides were then stained with eosin solution (Wako) for 10 s. Cells were visualized with Axio Imager A1 microscopes (Carl Zeiss). For immunohistochemistry, rehydrated paraffin-embedded tissue sections were stained with antibodies against GFP (Aves Labs), p-S6 (S235/236, #4858, Cell Signaling), and K_i-67 (BD Bioscience). Immunocomplexes were labeled using Alexa Fluor 488- or 546-conjugated antibodies. Sections were mounted using Prolong Gold antifade reagent with DAPI (Invitrogen), and analyzed by FV1000 confocal microscopy (Olympus).

1. Hoshii T, et al. (2012) mTORC1 is essential for leukemia propagation but not stem cell self-renewal. *J Clin Invest* 122(6):2114–2129.
2. Ventura A, et al. (2007) Restoration of p53 function leads to tumour regression in vivo. *Nature* 445(7128):661–665.
3. Tuveson DA, et al. (2004) Endogenous oncogenic K-ras(G12D) stimulates proliferation and widespread neoplastic and developmental defects. *Cancer Cell* 5(4):375–387.
4. Takahama Y, et al. (1998) Functional competence of T cells in the absence of glycosylphosphatidylinositol-anchored proteins caused by T cell-specific disruption of the Pig-a gene. *Eur J Immunol* 28(7):2159–2166.
5. Luche H, Weber O, Nageswara Rao T, Blum C, Fehling HJ (2007) Faithful activation of an extra-bright red fluorescent protein in "knock-in" Cre-reporter mice ideally suited for lineage tracing studies. *Eur J Immunol* 37(1):43–53.
6. Magee JA, et al. (2012) Temporal changes in PTEN and mTORC2 regulation of hematopoietic stem cell self-renewal and leukemia suppression. *Cell Stem Cell* 11(3): 415–428.
7. Kwiatkowski DJ, et al. (2002) A mouse model of TSC1 reveals sex-dependent lethality from liver hemangiomas, and up-regulation of p70S6 kinase activity in Tsc1 null cells. *Hum Mol Genet* 11(5):525–534.
8. Miyazaki M, et al. (2005) Polycomb group gene mel-18 regulates early T progenitor expansion by maintaining the expression of Hes-1, a target of the Notch pathway. *J Immunol* 174(5):2507–2516.
9. Agata Y, et al. (2007) Regulation of T cell receptor beta gene rearrangements and allelic exclusion by the helix-loop-helix protein, E47. *Immunity* 27(6):871–884.
10. Kawamoto H, et al. (2003) Extensive proliferation of T cell lineage-restricted progenitors in the thymus: An essential process for clonal expression of diverse T cell receptor beta chains. *Eur J Immunol* 33(3):606–615.

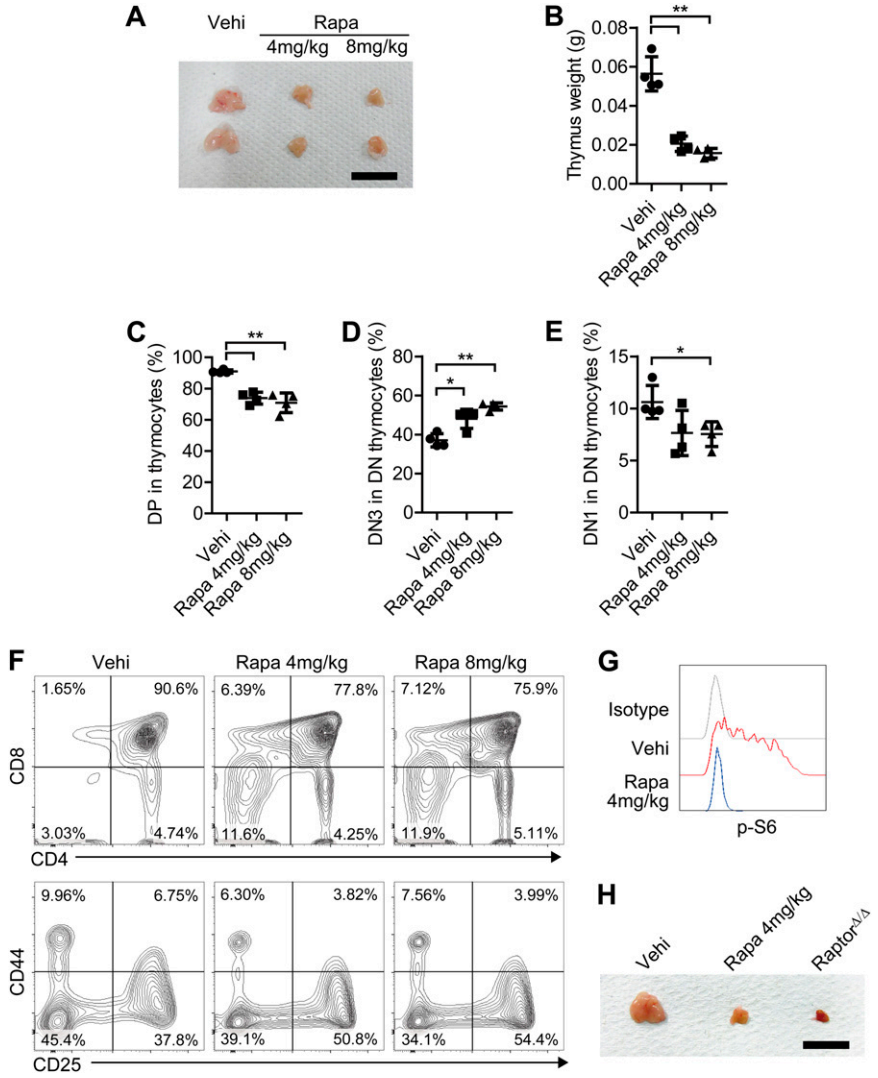

Fig. S1. The effect of rapamycin on T-cell development. (*A*) Representative morphology of thymuses from the vehicle-treated (Vehi), 4 mg/kg rapamycin-treated (Rapa 4 mg/kg), and 8 mg/kg rapamycin-treated (Rapa 8 mg/kg) mice. (*B*) Thymus weight of vehicle-treated and rapamycin-treated mice ($n = 4$). (*C*) The proportion of double-positive (DP) cells in vehicle-treated and rapamycin-treated thymocytes ($n = 4$). (*D*) The proportion of DN3 cells in vehicle-treated and rapamycin-treated DN-gated thymocytes ($n = 4$). (*E*) The proportion of DN1 cells in vehicle-treated and rapamycin-treated DN-gated thymocytes ($n = 4$). (*F*) Flow cytometric analyses of thymocytes from vehicle-treated and rapamycin-treated mice. Representative data from at least four individual experiments are shown. (*G*) Phosphorylation levels of S6 in DN cells in vehicle-treated (Vehi) and 4 mg/kg rapamycin-treated (Rapa 4mg/kg) mice. (*H*) Representative morphology of thymuses from the vehicle-treated (Vehi), 4 mg/kg rapamycin-treated (Rapa 4mg/kg), and *Raptor*-deficient (*Raptor*$^{\Delta/\Delta}$) mice described in Fig. 1*A*. For *B–E*, $*P < 0.05$, $**P < 0.01$ (Student *t* test).

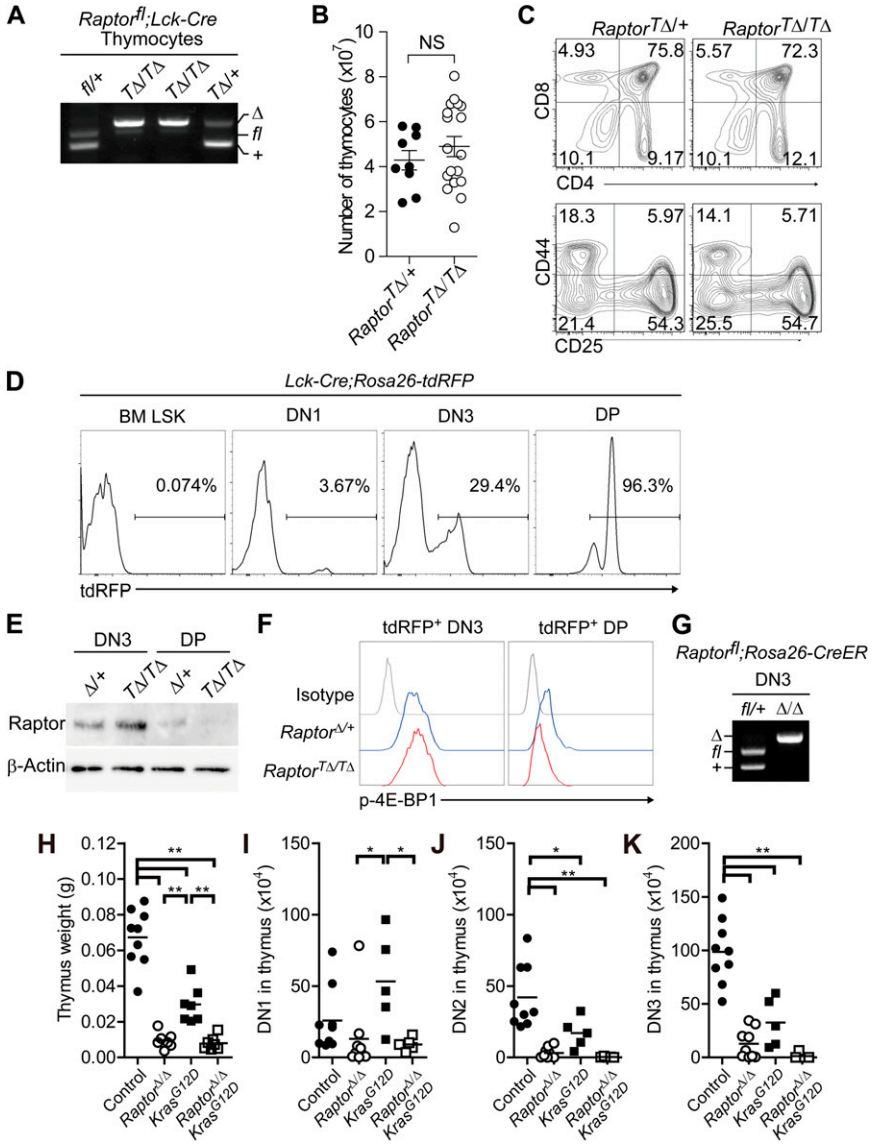

Fig. S2. *Raptor* deficiency in thymocytes. (*A*) Genotyping of thymocytes from *Raptor*^{fl}*Lck-Cre* mice. The wild-type *Raptor* allele (+), the floxed *Raptor* allele (*fl*), and the *Raptor* allele lacking exon 2 (Δ) were detected by PCR. (*B* and *C*) Number (*B*) and flow cytometric analyses (*C*) of thymocytes in *Raptor*$^{fl/+}$*Lck-Cre* mice (*Raptor*$^{TΔ/+}$, $n = 9$) and *Raptor*$^{fl/fl}$*Lck-Cre* mice (*Raptor*$^{TΔ/TΔ}$, $n = 18$). In *B*, the means ± SD are superimposed on the values from individual mice. (*D*) Tandem-dimer red fluorescent protein (tdRFP) expression in *Lck-Cre;Rosa26-tdRFP* mice. tdRFP fluorescence of LSK cells in BM LSK and T-cell subpopulations (DN1, DN3, and DP) in thymuses were examined. (*E*) Protein expression of Raptor in *Raptor*^{fl}*Lck-Cre* mice. tdRFP-positive DN3 and DP cells were collected from *Raptor*^{fl}*Lck-Cre* mice expressing a *Rosa26-tdRFP* reporter gene. (*F*) Phosphorylation levels of 4E-BP1 in tdRFP-expressing DN3 and DP cells from *Raptor*$^{Δ/+}$*;Lck-Cre;Rosa26-tdRFP* (*Raptor*$^{Δ/+}$) and *Raptor*$^{fl/fl}$*;Lck-Cre;Rosa26-tdRFP* (*Raptor* $^{TΔ/TΔ}$) mice. (*G*) Genotyping PCR using sorted DN3 cells from thymuses in mice with the indicated genotypes at 2 wk post-TAM. (*H*) Thymus weight from mice of the indicated genotypes ($n = 7$–9). Three *Raptor*$^{fl/fl}$ and six *Raptor*$^{fl/+}$*CreER* littermates were used as controls. (*I*–*K*) Absolute numbers of the indicated subpopulations in thymus ($n = 6$–9). For *B* and *H*–*K*, $*P < 0.05$, $**P < 0.01$ (Student *t* test). NS, not significant.

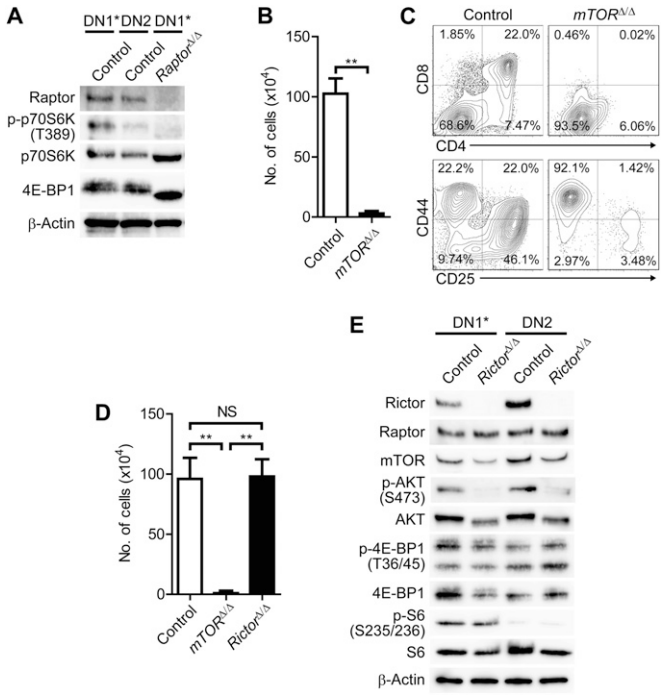

Fig. S3. mTORC1 and mTORC2 have distinct roles in the development of the earliest T-cell progenitors in vitro. (*A*) Phosphorylation of downstream targets of mTORC1. Lysates were prepared from the DN1* (DN1-like: DN $CD44^{+}CD25^{-}$) and DN2 (DN $CD44^{+}CD25^{+}$) populations shown in Fig. 1*F*. (*B* and *C*) $mTOR^{fl/fl}CreER$ LSK cells were cocultivated with TSt-4/DLL1 stromal cells for 16 d in the presence of 4-OHT in vitro. (*B*) Number of cells ($n = 4$ experiments). (*C*) Representative data from flow cytometric analyses. (*Lower*) DN cells. (*D*) $mTOR^{fl/fl}CreER$ or $Rictor^{fl/fl}CreER$ LSK cells were cocultivated with TSt-4/DLL1 stromal cells for 11 d in the presence of 4-OHT in vitro, after which the cells were counted ($n = 4$ experiments). (*E*) Phosphorylation of downstream targets of mTORC1 and mTORC2 in *Rictor*-deficient cells. Lysates were prepared from the indicated subpopulations after 11 d of cultivation. For *B* and *D*, $^{**}P < 0.01$ (Student *t* test). NS, not significant.

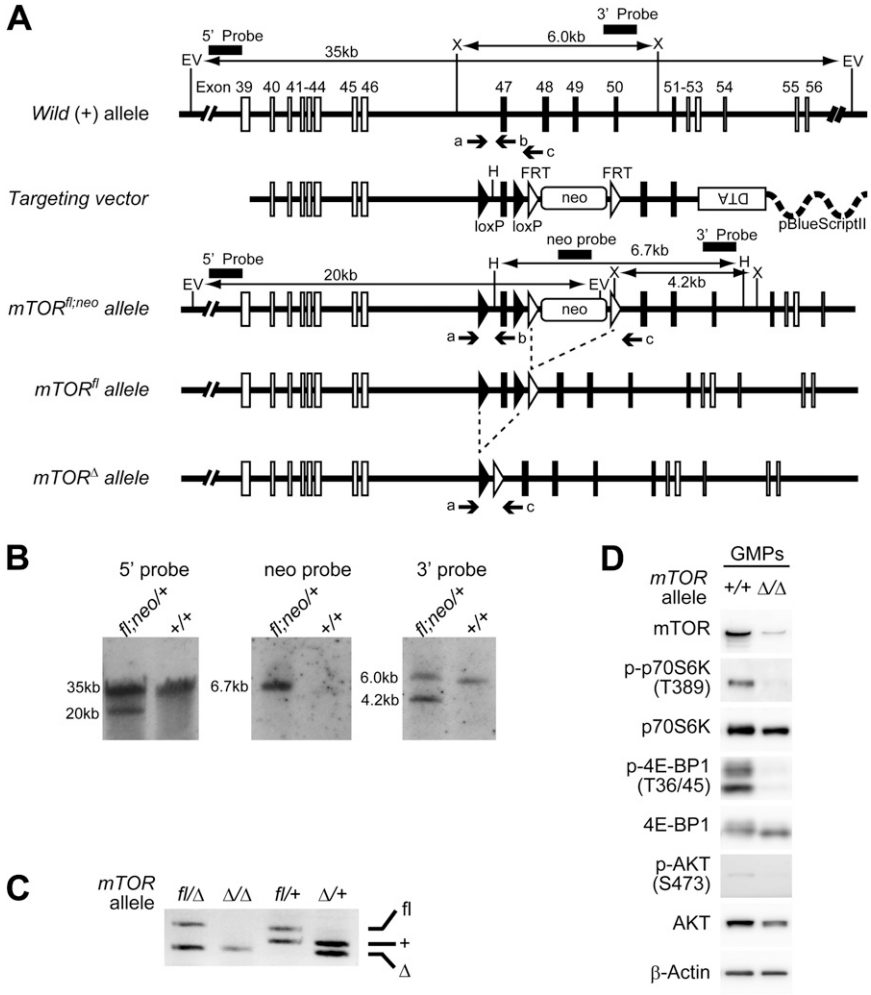

Fig. S4. Generation of *mTOR*^{flox} mice. (*A*) Targeting strategy to create the *floxed mTOR* allele. *mTOR* exon 47, a kinase domain-coding exon, is flanked by loxP sites. The targeting vector includes an FRT-flanked neo cassette (PGK promoter-driven neomycin resistance gene) for positive selection and a diphtheria toxin A (DTA) gene for negative selection. The neo cassette of the *mTOR*$^{fl;neo}$ allele was removed by crossing *mTOR*$^{fl;neo}$ mice with *CAG-Flp* mice. Probes for Southern blotting (5′ probe, neo probe, 3′ probe) and primers for PCR (a, b, c) are indicated. EV, EcoRV; X, XbaI; H, HindIII. The exons of the *mTOR* gene (exons 39–56) are indicated by open and filled boxes. Filled boxes (exons 47–51) indicate exons encoding the kinase domain of mTOR. (*B*) Southern blot confirming the recombination of the targeting vector at the mTOR genomic locus. ES clone DNA was digested by EcoRV, XbaI, or HindIII and hybridized to a digoxigenin-labeled 5′ probe, neo probe, or 3′ probe, respectively. (*C*) Genotyping of mouse tail DNA by PCR. The wild-type *mTOR* allele (+), the floxed *mTOR* allele after excision of the Neo cassette (*fl*), and the *mTOR* allele lacking exon 47 (Δ) were detected by combinations of the primers (a, b, c) indicated in *A*. (*D*) Phosphorylation of downstream targets of mTOR in *mTOR*$^{+/+}$*CreER* or *mTOR*$^{fl/fl}$*CreER* (Δ/Δ) GMP 2 wk post-TAM. β-Actin, loading control.

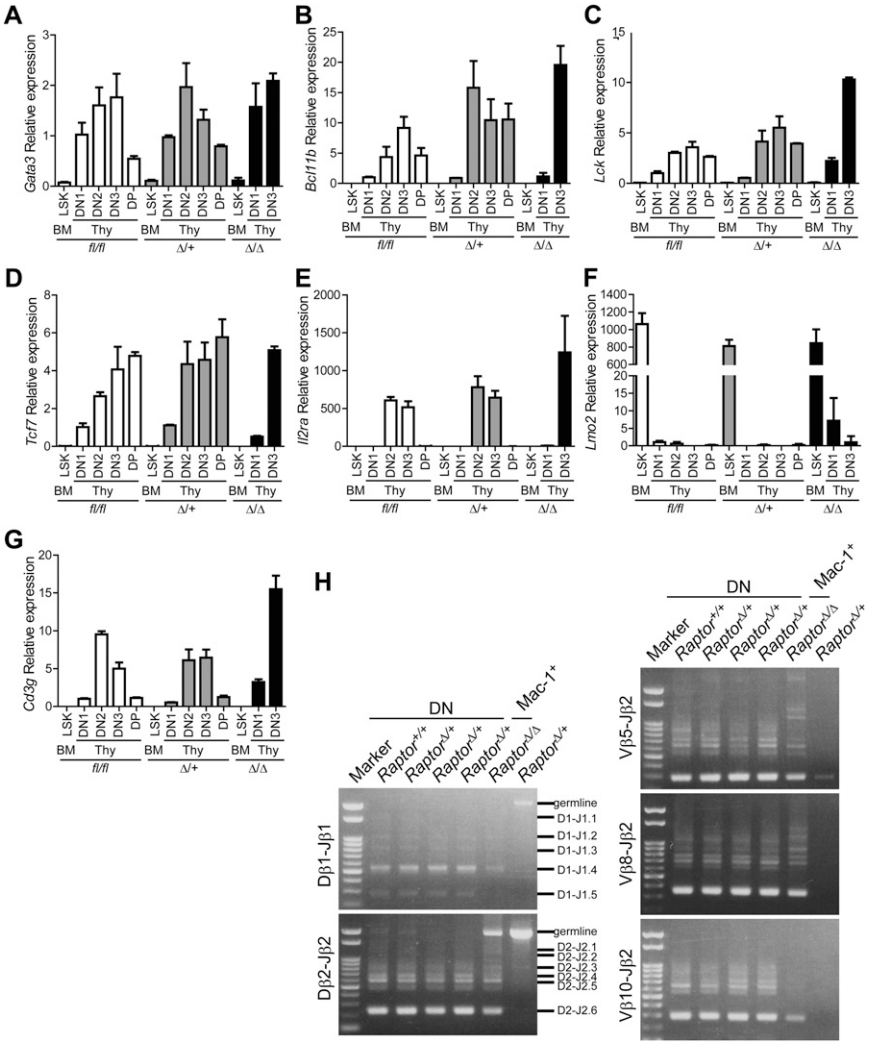

Fig. S5. Gene expression profiles of *Raptor*-deficient T-cell progenitors. (*A*–*G*) mRNA expression of lineage-specific genes in BM LSK cells and thymic DN1, DN2, DN3, and DP cells. TaqMan probes for the indicated genes were used, and results were normalized to β-actin transcripts ($n = 3$). (*H*) TCRβ gene rearrangement in DN cells. Genomic DNA samples were isolated from mice with the indicated genotypes. BM Mac-1+ cells were analyzed as a nonrearranged control.

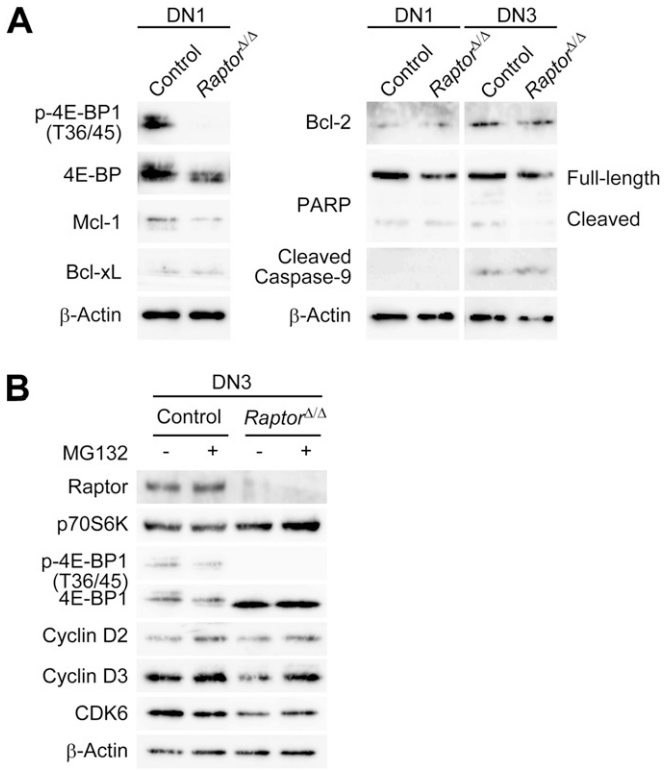

Fig. S6. Expression of genes related to apoptosis, survival, and the cell cycle in *Raptor*-deficient T-cell progenitors. (*A*) Protein expression of phospho-4E-BP1, survival-related (Mcl-1, Bcl-xL, Bcl-2), and apoptosis-related (cleaved PARP, cleaved caspase-9) proteins in DN1 and DN3 T-cell progenitors from *Raptor*-deficient mice at 2 wk post-TAM. (*B*) Protein amount of Cyclin D2/D3 and CDK6 in the absence or presence of the proteasome inhibitor MG-132. DN3 cells from in vitro culture were analyzed 2 h after MG-132 administration.

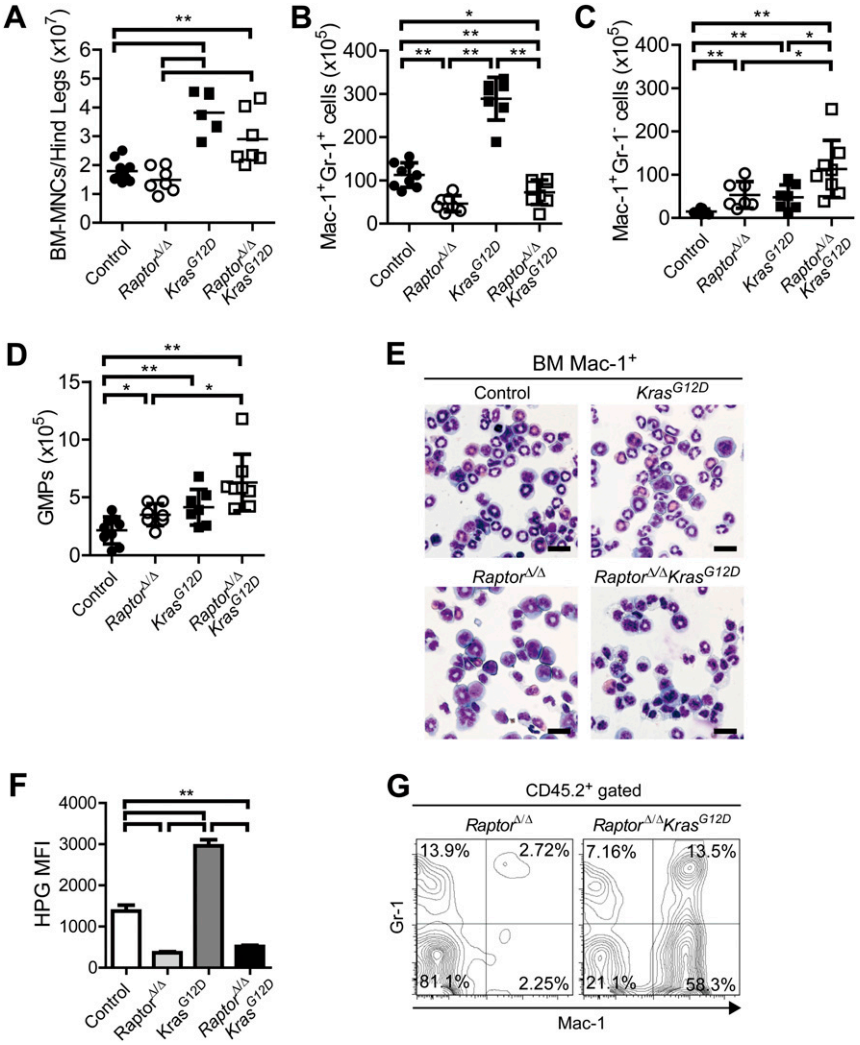

Fig. S7. Characterization of *Raptor*$^{\Delta/\Delta}$*Kras*^{G12D} myeloid progenitors. (*A*) Numbers of BM-MNCs in the hind legs (femurs and tibias) of mice with the indicated genotypes. Values were measured at 2 wk post-TAM (n = 7–10). (*B–D*) Absolute numbers of indicated subpopulations in the hind legs are shown (n = 7–9). Horizontal lines are mean values. (*E*) Morphological analysis of Mac-1$^+$ myeloid cells. Mac-1$^+$ cells from the BM of the indicated mice were stained with May-Grünwald-Giemsa. The number of mature granulocytes with ring-shaped nuclei was strongly reduced by *Raptor* deficiency. (*F*) Protein synthesis assay. Sorted Lineage$^-$Sca-1$^-$c-KIT$^+$ cells were labeled with HPG (L-homopropargylglycine: amino acid analog of methionine). The graph shows median fluorescence intensity (MFI) of HPG-Alexa Fluor 488 in three independent experiments. (*G*) Flow cytometric analysis of PB cells, which showed an increased white blood cell (WBC) count in recipient mice bearing *Raptor*$^{\Delta/\Delta}$ cells or *Raptor*$^{\Delta/\Delta}$*Kras*^{G12D} cells. *A–D* and *F*: $^*P < 0.05$, $^{**}P < 0.01$ (Student t test).

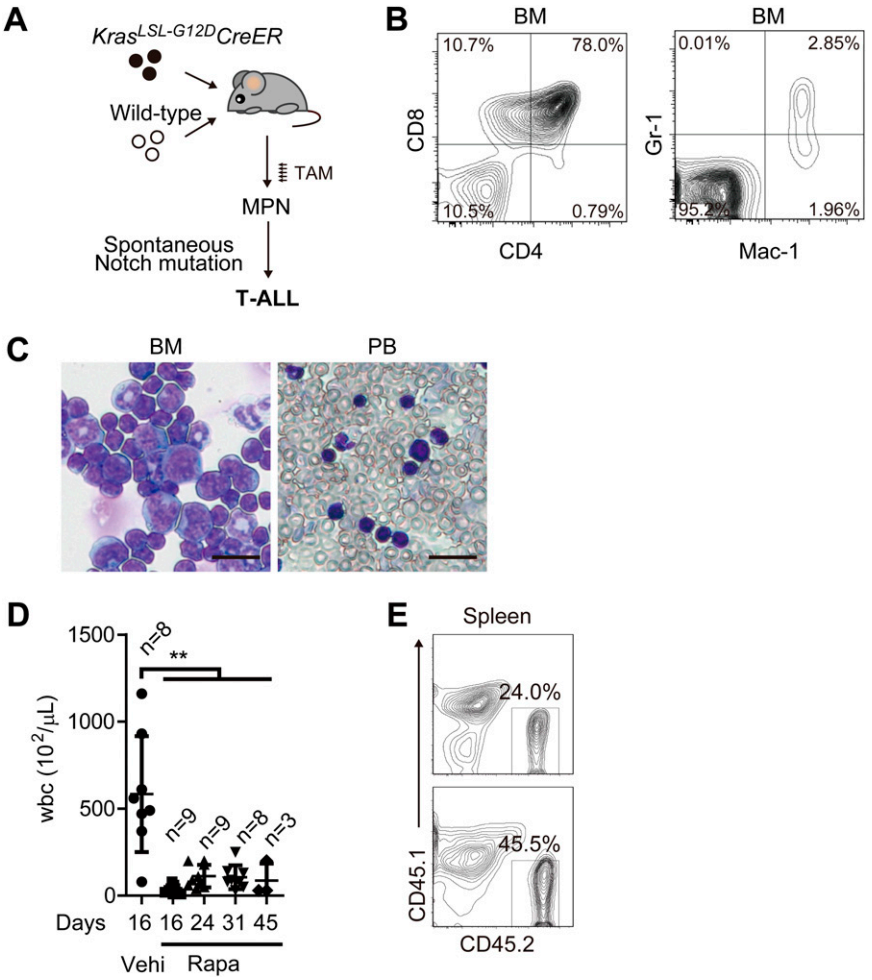

Fig. S8. Establishment of oncogenic Kras-induced T-ALL. (*A*) Experimental design for establishment of oncogenic Kras-evoked T-ALL cells. (*B*) Flow cytometric analyses of BM at the endpoint (84 d post-TAM). (*C*) Morphological analysis of BM and PB cells. BM cells and PB cells at the end-point were stained with May-Grünwald-Giemsa. (*D*) Number of WBCs in PB from recipient mice bearing $Kras^{G12D}$ T-ALL cells after vehicle or rapamycin treatment. $^{**}P < 0.01$ (Student *t* test). (*E*) Flow cytometric analysis of BM-MNCs and splenic MNCs from vehicle- or rapamycin-treated mice bearing oncogenic Kras-induced T-ALL cells. Cells were collected 3 wk after transplantation.

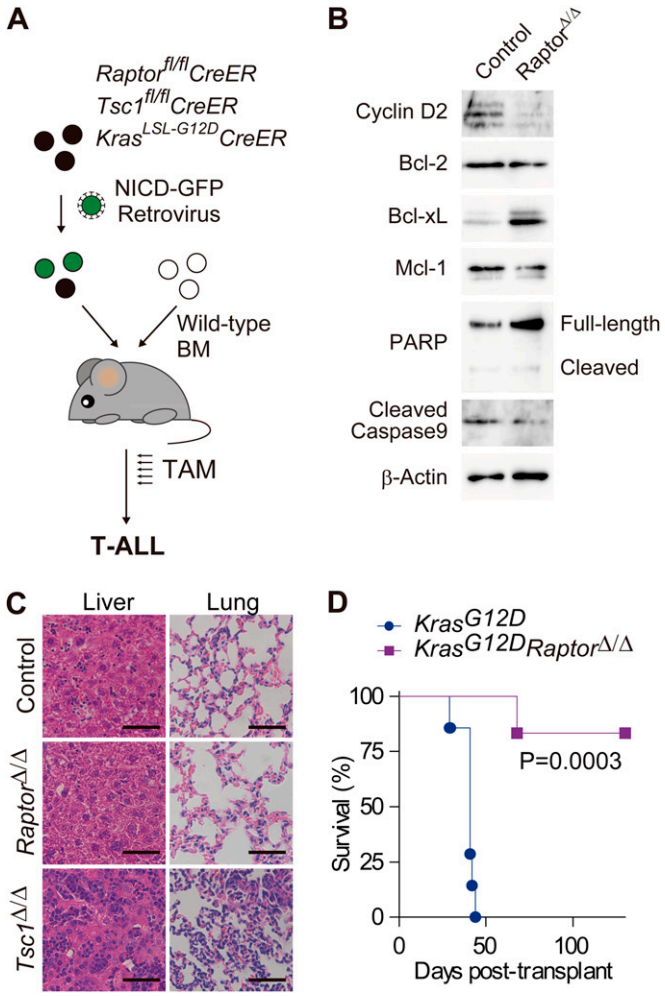

Fig. S9. Expression of Cyclin D2 and apoptosis- and survival-related genes in *Raptor*-deficient T-ALL cells. (*A*) Experimental design for NICD-GFP–transduced T-ALL model. (*B*) Protein expression of Cyclin D2, survival-related (Mcl-1, Bcl-xL, Bcl-2), and apoptosis-related (cleaved PARP, cleaved caspase-9) proteins in *Raptor*-deficient GFP+ T-ALL cells from T-ALL mice at 5 d post-TAM. (*C*) Histology of liver and lung from recipient mice bearing NICD-GFP–transduced cells. Samples were obtained 39 d posttransplant. (Scale bars, 50 μm.) (*D*) Survival of recipient mice bearing NICD-GFP–transduced $Kras^{G12D}$ and $Raptor^{\Delta/\Delta}Kras^{G12D}$ cells. *P* value, log-rank test.